International Journal of Information, Control and Computer Sciences
ISSN: 2517-9942
Vol:14, No:5, 2020

Dual-Polarized Multi-Antenna System for Massive MIMO Cellular Communications

Naser Ojaroudi Parchin, Haleh Jahanbakhsh Basherlou, Raed A. Abd-Alhameed, Peter S. Excell

Abstract**—**In this paper, a multiple-input/multiple-output (MIMO) antenna design with polarization and radiation pattern diversity is presented for future smartphones. The configuration of the design consists of four double-fed circular-ring antenna elements located at different edges of the printed circuit board (PCB) with an FR-4 substrate and overall dimension of 75×150 mm^2. The antenna elements are fed by 50-Ohm microstrip-lines and provide polarization and radiation pattern diversity function due to the orthogonal placement of their feed lines. A good impedance bandwidth ($S_{11} \leq$ -10 dB) of 3.4-3.8 GHz has been obtained for the smartphone antenna array. However, for $S_{11} \leq$ -6 dB, this value is 3.25-3.95 GHz. More than 3 dB realized gain and 80% total efficiency are achieved for the single-element radiator. The presented design not only provides the required radiation coverage but also generates the polarization diversity characteristic.

Keywords**—**Cellular communications, MIMO systems, mobile-phone antenna, polarization diversity.

I. Introduction

MIMO technology can exponentially increase the data transfer rate and spectrum efficiency without any need of increasing the transmission power and bandwidth [1]-[4]. It is the most promising technology to be used in the upcoming 5G communications [5]-[8]. To be more accurate, the fourth generation (4G) smartphones are set to use the long term evolution (LTE) MIMO technology and operate in multi-bands. MIMO antennas are to use in future portable devices such as mobile handsets and tablets [9]-[12]. Unlike the standard MIMO systems which employ two or four elements in a single physical package, a high number of antenna radiators are employed for the massive MIMO system.

In accordance with the requirement of mobile networks, low-profile, wideband antenna elements with sufficient mutual couplings are an urgent demand in the 5G terminals for handheld device applications [13]-[16]. Since the space of the portable device is limited, the configuration of the multiple antennas is difficult to install in such a limited device. Thus, integration of multiple antenna elements into a mobile handset is a new challenge. Recently, several techniques have been introduced to design MIMO antennas for 4G and sub-6 GHz 5G mobile terminals [17]-[20]. However, these smartphone antennas not only exhibit narrow impedance-bandwidth (either single-band or dual/multi-bands), but also employ single-polarized resonators mainly with uniplanar structures occupying large spaces of the mainboard which could increase the complexity of the system.

In this study, a design of MIMO smartphone antenna with compact radiation elements, high efficiency, and wide bandwidth is presented for 3.6 GHz 5G applications. 3.6 GHz is a candidate frequency band for sub-6-GHz 5G cellular networks, proposed by Ofcom [21]. Four elements of double-fed/differently-polarized circular-ring/slot-line antennas are deployed at different corners to exhibit orthogonal polarizations with the pattern and polarization diversity. The proposed antenna system exhibits not only sufficing radiation coverage supporting different sides of the mainboard but also the polarization diversity [22], [23].

The configuration of the antenna element consists of a compact circular-ring slot radiator with a pair of microstrip feed lines. The antenna elements exhibit 400 MHz impedance bandwidth with low mutual coupling function for $S_{11} \leq$ -10 dB. High isolation (15 dB), high efficiency (60%-80%), wide bandwidth (400 MHz), and dual-polarized properties have been achieved for the proposed design. The CST software was used to investigate antenna characteristics and to find the optimal structure for the antenna [24].

II. Characteristic of Single-Element Antenna

The configuration of the designed dual-polarized circular-ring antenna is illustrated in Fig. 1. It is designed on an FR-4 substrate (h = 1.6 mm, ε = 4.4, and δ = 0.025) to operate at 3.6 GHz. Its design parameters (in mm) are as follow: W_S = 34, L_S = 34, h_S = 1.6, W_f = 3, L_f = 11.5 r = 9.25, and r_1 = 8

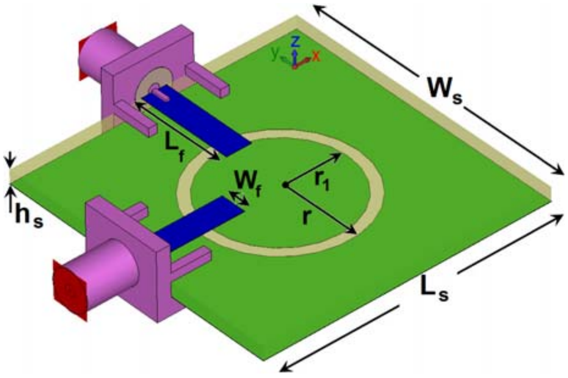

Fig. 1 Configuration of the dual-polarized slot antenna element

The antenna configuration contains a pair of microstrip

Naser Ojaroudi Parchin* and Raed A. Abd-Alhameed are with the Faculty of Engineering and Informatics, University of Bradford, Bradford BD7 1DP, UK (*e-mail: N.OjaroudiParchin@Bradford.ac.uk).
Haleh Jahanbakhsh Basherlou is with the Bradford College, Bradford, West Yorkshire, BD7 1AY, UK.
Peter S. Excell is with the Engineering Division, Glyndwr University, Wrexham LL11 2AW, UK.

feed lines along with a circular-ring slot radiator in the ground plane. Fig. 2 illustrates the antenna S-parameters. From the above observations, it is clear that for $S_{11} \leq$ -10 dB, the antenna provides 400 impedance bandwidth (3.4-3.8 GHz). In addition, the mutual coupling characteristic of the dual-port design is less than -15 dB at the antenna resonance frequency (3.6 GHz).

The current distributions in the ground plane of the antenna at operating frequency (3.6 GHz) are illustrated in Fig. 3. The currents are mainly distributed around the slot-ring radiator. As can be observed from Figs. 3 (a) and (b), for the different feeding ports of the antenna, the current floww are equal and opposite due to the polarization diversity function [25], [26]. Fig. 4 represents the antenna 3D radiation pattern for each feeding port: the antenna exhibits similar radiation patterns with more than 3 dB realized gain and different polarizations from the feeding ports. The fundamental characteristics in terms of radiation efficiency, total efficiency, maximum gain, and directivity over the antenna operation band are shown in Fig. 5.

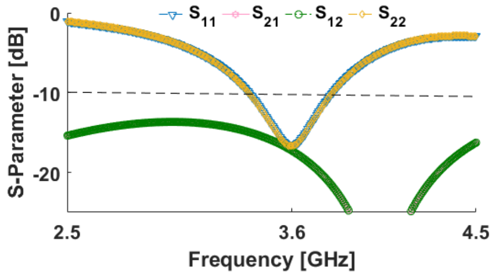

Fig. 2 S-parameter results of the single-element antenna design

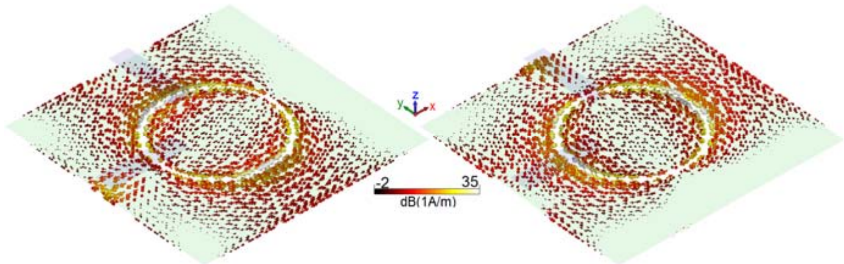

(a) (b)

Fig. 3 Current densities at 3.6 GHz for (a) Port 1 and (b) Port 2

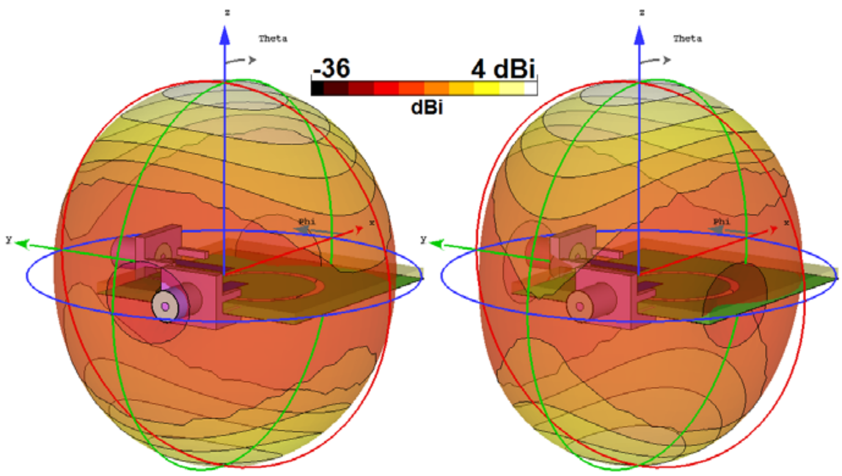

(a) (b)

Fig. 4 (a) 3D radiation patterns at 3.6 GHz for (a) Port 1 and (b) Port 2

As shown the antenna provides very high efficiencies. More than 75% radiation and total efficiencies have been achieved over the entire operation band. Besides, the antenna has more than 80% efficiency at the operating frequency (3.6 GHz). According to the obtained results, the antenna provides almost constant maximum gain characteristics over its operation band. Around 3-3.5 dBi maximum gain has been achieved for the antenna.

III. Multiple-Antenna System

Fig. 6 illustrates the schematic of the MIMO antenna design for future smartphones. The design has been implemented on an FR4 substrate (h: 1.6 mm, ε: 4.4, and δ: 0.025) with the size of $75 \times 150 \times 1.6$ mm^3. As illustrated, four elements of the dual-polarized radiators have been placed at the corner of the PCB. Each pair of microstrip lines will excite orthogonal polarizations to enhance the MIMO performances of the design.

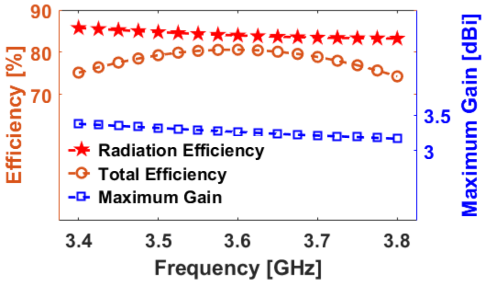

Fig. 5 Fundamental characteristics of the antenna element

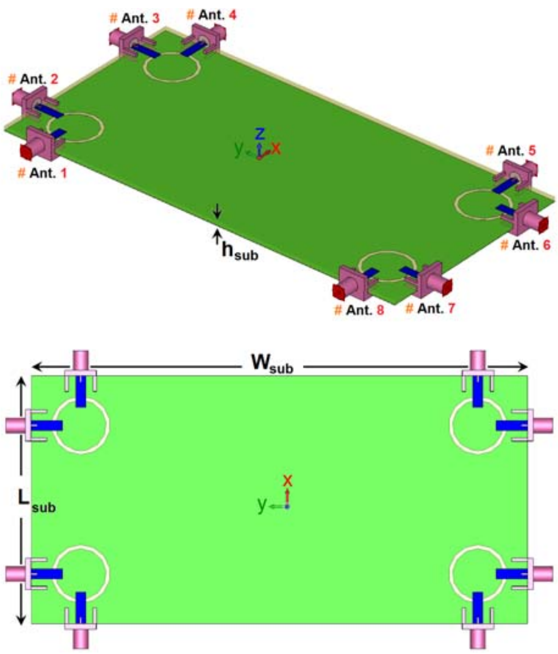

Fig. 6 Side and top vies of the proposed MIMO antenna system

Fig. 7 depicts the antenna S parameters (including S_{nn} and S_{mn}) over the antenna operation band. The smartphone 5G antenna exhibits good S parameters with wide bandwidth (3.4-3.8 GHz) and acceptable isolations of better than 15 dB. It is evident that the dual-polarized radiation elements provide similar performances. The design radiation patterns are displayed in Fig. 8: the antenna elements have quasi-omnidirectional radiation patterns that mainly cover the top and bottom sides of the smartphone PCB. Due to this point, the ring-slot antenna is a better candidate to be used in smartphone antenna design, compared with other microstrip antennas such as patch, dipole, and Yagi antennas. In addition, the antenna elements are miniaturized and providing double-fed/dual-polarization function. As can be observed, each side of the PCB has been covered with differently polarized radiation patterns. Thus, the smartphone antenna system exhibits a full radiation coverage and can support both vertical and horizontal polarizations which make it suitable for future smartphone applications [27], [28]. Moreover, high radiation and total efficiencies are observed within the frequency band of the MIMO antenna system, as shown in Fig. 9: more than 75% radiation and total efficiencies have been obtained for the radiation elements at 3.6 GHz. The smartphone MIMO antenna is constructed on a cheap FR4 substrate with an overall dimension of 75×150×1.6 mm^3. Top and bottom views of the prototype are shown in Figs. 10 (a) and (b), respectively.

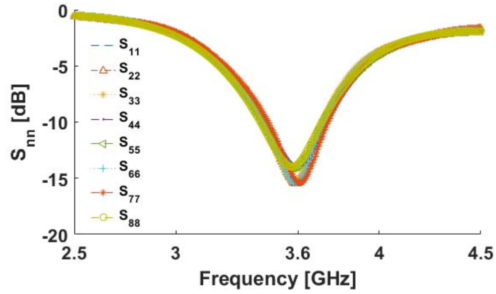

(a)

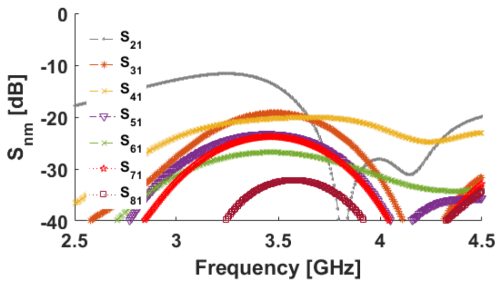

(b)

Fig. 7 Simulated (a) S_{nn} and (b) S_{mn} of the MIMO design

Figs. 11 (a) and (b) illustrate measured/simulated S-parameters (S_{11}~S_{88} and S_{21}~S_{81}) of the design. As illustrated, the circular-ring slot resonators achieve good S-parameters with sufficient impedance bandwidth and low mutual coupling characteristic in the desired frequency range [29], [30]. There is some deflection from the measurements and simulations which could be mainly because of the errors in fabrication, feeding and measurements processes.

IV. Conclusion

A design of MIMO antenna with orthogonally dual-polarized radiators is presented for 5G smartphone applications. Its configuration contains eight-port/four elements of modified circular-rings slot radiators deployed at four edges of the mobile-phone PCB. The operation frequency of the radiators spans from 3.4 to 3.8 GHz with the resonance at 3.6 GHz. Fundamental properties of the smartphone antenna design including S-parameter, efficiency, radiation patterns, and antenna gain are investigated. The MIMO antenna design not only can provide full radiation coverage but also it can support different polarizations. A prototype of the designed MIMO antenna was fabricated and its measured results are provided. It is simple and easy for fabrication using printed circuit technology. The results demonstrated that the antenna meets the requirements for use in smartphones.

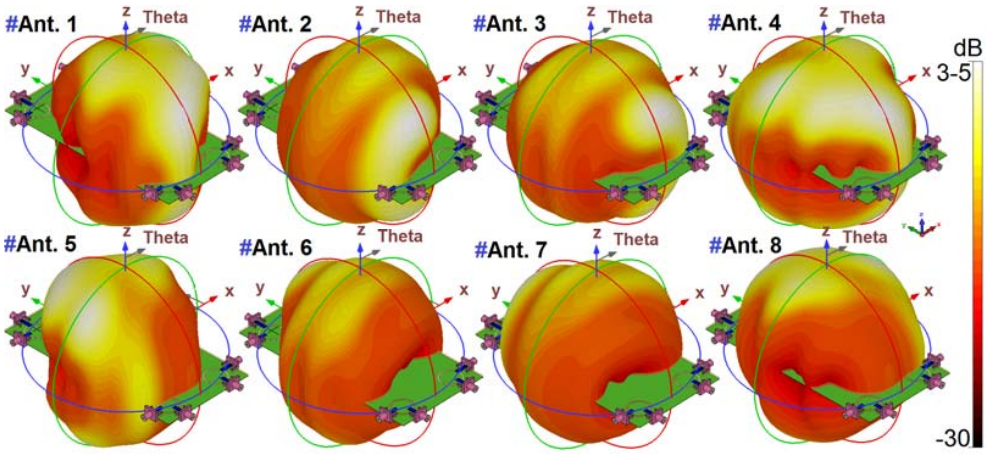

Fig. 8 Radiation patterns of the proposed MIMO antenna system

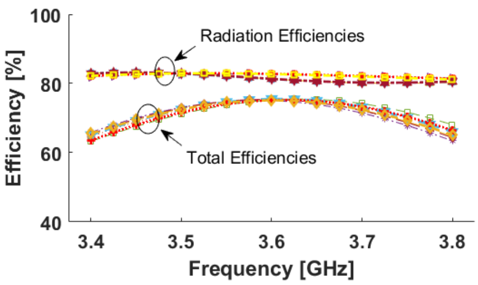

Fig. 9 Efficiencies of the MIMO antenna

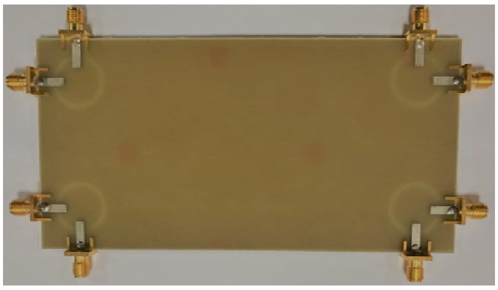

(a)

(b)

Fig. 10 (a) Top and (b) bottom vies of the fabricated prototype

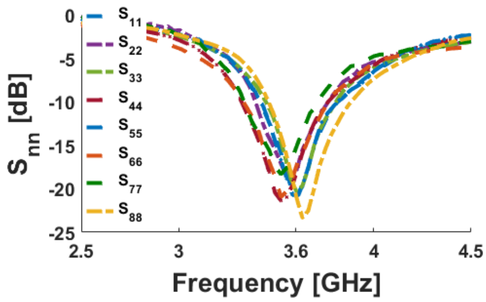

(a)

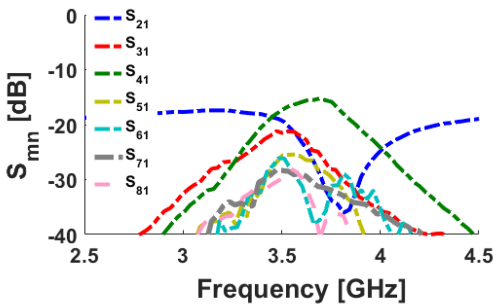

(b)

Fig. 11 Measured (a) S_{nn} and (b) S_{mn} of the MIMO design.

ACKNOWLEDGMENT

This work is supported by the European Union's Horizon 2020 research and innovation programme under grant agreement H2020-MSCA-ITN-2016 SECRET-722424.

REFERENCES

[1] M. S. Sharawi, "Printed MIMO antenna engineering," Norwood, MA, USA: Artech House, 2014.

[2] N. O. Parchin, et al., "8×8 MIMO antenna system with coupled-fed elements for 5G handsets," The IET Conference on Antennas and

Propagation (APC), 11-12 November, 2019, Birmingham, UK.
[3] N. O. Parchin, et al., “Dual-polarized MIMO antenna array design using miniaturized self-complementary structures for 5G smartphone applications,” EuCAP Conference, Krakow, Poland, 2019.
[4] N. Ojaroudi et al., “Design of CPW-fed slot antenna for MIMO system applications,” Microw. Opt. Technol. Lett., vol. 56, pp. 1278-1281, 2014.
[5] A. Osseiran, et al., “Scenarios for 5G mobile and wireless communications: the vision of the METIS project,” IEEE Commun. Mag., vol. 52, pp.26-35, 2014.
[6] Q.U.A. Nadeem, et al., “Design of 5G full dimension massive MIMO systems,” IEEE Trans. Commun., vol. 66, pp. 726–740, 2018.
[7] N. Ojaroudiparchin, et al., “Multi-layer 5G mobile phone antenna for multi-user MIMO communications,” TELFOR 2015, Nov.2015, Serbia.
[8] N. O. Parchin, et al., “MM-wave phased array quasi-yagi antenna for the upcoming 5G cellular communications,” Applied Sciences, vol. 9, pp. 1-14, 2019.
[9] N. Ojaroudi, et al., “An omnidirectional PIFA for downlink and uplink satellite applications in C-band,” Microwave and Optical Technology Letters, vol. 56, pp. 2684-2686, 2014.
[10] Y.-L. Ban, et al., “4G/5G multiple antennas for future multi-mode smartphone applications,” IEEE Access, vol. 4, pp. 2981–2988. 2016.
[11] P. Gupta, “Evolvement of mobile generations: 1G to 5G,” International Journal for Technological Research in Engineering, vol. 1, pp. 152-157, 2013.
[12] N. Ojaroudi, “Design of microstrip antenna for 2.4/5.8 GHz RFID applications,” GeMic 2014, RWTH Aachen University, Germany, 2014.
[13] N. Ojaroudi, “Circular microstrip antenna with dual band-stop performance for ultra-wideband systems,” Microw. Opt. Technol. Lett., vol. 56, pp. 2095-2098, 2014.
[14] N. Ojaroudi, et al., “Very low profile ultrawideband microstrip band-stop filter,” Microw. Opt. Technol. Lett., vol. 56, pp. 709-711, 2014.
[15] N. O. Parchin, et al., “Mobile-phone antenna array with diamond-ring slot elements for 5G massive MIMO system,” Electronics, vol. 9, pp. 1-14, 2019.
[16] N. Ojaroudi, et al., “Compact ultra-wideband monopole antenna with enhanced bandwidth and dual band-stop properties,” International Journal of RF and Microwave Computer-Aided Engineering, vol. 25, pp. 346–357, 2015.
[17] M.-Y. Li, et al., “Tri-polarized 12-antenna MIMO array for future 5G smartphone applications,” IEEE Access, vol. 6, pp. 6160–6170, 2018.
[18] R. Hussain, et al., “4-element concentric pentagonal slot-line-based ultra-wide tuning frequency reconfigurable MIMO antenna system,” IEEE Trans. Antennas Propag., vol. 66, pp. 4282–4287, 2018.
[19] M. Abdullah, et al., “Eight-element antenna array at 3.5GHz for MIMO wireless application,” PIER C, vol. 78, pp. 209-217, 2017.
[20] Y. Li, et al., “High-isolation 3.5-GHz 8-antenna MIMO array using balanced open slot antenna element for 5G smartphones,” IEEE Trans. Antennas Propag., 2019, doi:10.1109/TAP.2019.2902751.
[21] Statement: Improving Consumer Access to Mobile Services at 3.6 GHz to 3.8 GHz. Available online: https://www.ofcom.org.uk/consultations-and-statements/category-1/future-use-at-3.6-3.8-ghz.
[22] N. Ojaroudi, et al., “Enhanced bandwidth of small square monopole antenna by using inverted U-shaped slot and conductor-backed plane,” ACES Journal, vol. 27, 685– 690, 2012.
[23] N. O. Parchin et al., “Multi-band MIMO antenna design with user-impact investigation for 4G and 5G mobile terminals, Sensors, vol. 19, pp. 1-16, 2019.
[24] CST Microwave Studio, ver. 2017, CST, Framingham, MA, USA, 2017.
[25] N. O. Parchin, “Low-profile air-filled antenna for next generation wireless systems,” Wireless Personal Communications, vol. 97, pp. 3293–3300, 2017.
[26] P. Salonen, et al., “A small planar inverted-F antenna for wearable applications”, IEEE International Symposium on Wearable Computers, pp. 96- 100, 1999.
[27] A. Zhao, R. Zhouyou, “Size reduction of self-isolated MIMO antenna system for 5G mobile phone applications,” IEEE Antennas and Wireless Propagation Letters, vol. 18, pp. 152-156, 2019.
[28] N. Ojaroudi, “Design of ultra-wideband monopole antenna with enhanced bandwidth,” 21th Telecommunications Forum, TELFOR 2013, 27 – 28 November, 2013, Belgrade, Serbia.
[29] A. Musavand, et al., “A compact UWB slot antenna with reconfigurable band-notched function for multimode applications,” Appl Comp Electromagn Soc J, vol. 31, pp. 14-18, 2016.
[30] A. Ullah, et al., “Coplanar waveguide antenna with defected ground structure for 5G millimeter wave communications,” IEEE MENACOMM'19, Bahrain, 2019.